

Immersion Calorimetric Method to Study Lime Surfaces Impurities and Particles Aggregate Morphologies

Dario T. Beruto^{*1}, Rodolfo Botter², Alberto Lagazzo³

DICCA (Department of Civil, Chemical and Environmental Engineering), University of Genoa, P.le J.F. Kennedy (Fiera del Mare), Pad. D, 16129 – Genoa, Italy

^{*1}dabe@unige.it; ²rodolfo.botter@unige.it; ³alberto.lagazzo@unige.it

Abstract

A new application of the immersion calorimetric method has been developed to study the specific wetting heat of colloidal lime particles dispersed in liquid paraffin. This method, combined with SEM, EDAX and Hg porosimeter measurements, allows to evaluate the effects of the limestone impurities on the shape of the limes particles aggregates. These morphologies are dependent upon the limestone thermal decomposition conditions and upon the impurities of the limestone rocks. The impurities that influence the shape of individual and agglomerated limes particle, according to this study, are SiO₂ and Al₂O₃, in percentages at least of 0.24 wt% and 0.12 wt% respectively. At the temperature of 1300°C these oxides, combined with CaO, they can form a viscous liquid-like phase that changes dramatically the shape of the lime particles. Rhombohedra or irregular grains of about 0.4–3 µm, change their shape into flat and large crystallites of 10×10×1 µm. For the platelet microstructure, the specific exothermic heat ξ [J/m²] is equal to -8 ± 2 J/m², while, for the aggregates of rhombohedric grains, is in the average -0.9 ± 0.1 J/m².

From a technological point of view this study can be used to optimise the thermal decomposition conditions of limestone rocks with a proper content of silica and alumina oxides.

Keywords

Lime; Limestone; CaCO₃/CaO; Alumina Impurity; Silica Impurity; Particles Morphology; Decomposition

Introduction

In a previous paper [1], we developed a consecutive decomposition-sintering dilatometer method (CDSD) to study the effect of impurities on the lime microstructures formed during the decomposition of limestone in air. It had been proven that at temperatures from 700–1200°C, the grains of CaO-based limes can have different morphologies as a consequence of the thermodynamic and kinetic features of the calcium carbonate decomposition processes [2–4]. It is well known [5–7] that the partial pressure of the CO₂ escaping from the interfaces during CaO/CaCO₃ reactions has an effect on the microstructure of the obtained CaO grains. The impurities that transfer from the limestone rocks to the lime may contribute to this phenomenon with complex mechanisms [8–10]. To shed some light in this rather difficult field is a very important topic since the limestone impurities are a sort of kit that geological history has left in the limestone matrix [11] that might be used to obtain limes with optimal properties for saving energy problems and CO₂, SO₂/SO₃ capture [12–16].

In this paper, we investigate further these issues by developing a new method based on the immersion calorimetric technique [17]. This method had been applied by others authors [18, 19] to obtain information on the nature of the surface chemical and physical properties of colloidal particles dispersed in a selected liquid phase. In one of our recent papers [20], we studied the dispersions of silica and kaolin powders in liquid paraffin as a function of their solid volume fraction and we proved that the corresponding exothermic wetting heat and/or the specific wetting heat ξ (J/m²) can account for the network formed by the particle aggregates in the dispersing liquid. The application of these principles to the colloidal CaO-paraffin system allows to discuss the solid-liquid interfaces, only in term of van der Waals and steric forces, due to the absence of aromatic and/or of naphthenic groups in the paraffin chains [21]. On this ground the specific wetting heat that gives an indication of the dispersion stability [18],

very reasonably, is mainly dependent upon the accessibility of the paraffin molecules to the lime aggregate surfaces and/or to the lime grain boundaries. Accordingly any effect due to the impurities in changing the limes particles and/or the aggregate microstructure should be detected by the corresponding changes in their specific exothermic wetting heat.

From a technological point of view this method, which is at the best of our knowledge a new approach, can be coupled with SEM, EDAX and chemical analysis to provide a rather complete framework to study the physical and chemical nature of lime particle surface as affected by the limestones impurities.

Experimental

Materials

Limestone rocks from different sources with the chemical compositions reported in Tab. 1 are used throughout this paper to obtain the corresponding limes via thermal decomposition at temperatures between 980 and 1300°C in air.

It can be observed that these limestones have a high calcium carbonate content that ranges between 99.4% and 100% by weight, which corresponds to a CaO mol fraction % ranging between 98.3% and 100 %. For all limestones, MgO is the primary impurity despite never exceeding 1%. LMST1 has a silica and alumina content greater than the other limestones.

High purity liquid paraffin obtained from Carlo Erba without the aromatic and naphthenic groups (0.88 g/cm³, boiling temperature of 68°C, ignition point of 135°C and viscosity of 20 mPas) were used as the liquid phase for the wetting experiments. When solid particles, previously heat-treated in vacuum, are brought into contact with a pure wetting liquid the solid-liquid interactions can be

Methods

1) Powder Preparation

Limestone pebbles 5–15 mm in diameter were decomposed at a constant temperature between 980–1300°C in air for 2 h and 30 min. The complete decomposition was confirmed by weight loss. The obtained limes had an average size between 1–8 µm. For some of these samples, a chemical analysis of the impurities was performed.

Reagent grade (r.g.) CaCO₃ powders were decomposed at 900°C for 30 mins and 1350°C for 4 hours to obtain small surface CaO samples for comparison. All of the CaO-based oxides were stored in sealed containers in a desiccator. All the samples were been decomposed in air.

2) Calorimetric Measurements

Calorimetry tests were performed to measure the heat of dispersion in liquid paraffin [17, 20, 22] of the CaO-based oxides.

A Setaram C80 calorimeter described in a recent paper [20] and equipped with stainless steel wetting cells were used in these experiments. Two identical cells (measure and reference) were placed in the calorimetric block at a temperature of 30±0.01°C. Each cell consisted of a cylinder (2 cm in diameter and 10 cm in height) with a mobile piston inside.

Approximately 200 mg of powdered lime was introduced for the calorimetric tests in liquid paraffin using a homemade glass ampoule. This ampoule resembled a cylindrical container 5 mm in diameter with a narrowing hook at one end to facilitate breaking. The open ampoule was filled with the sample and connected to a mechanical vacuum system before sealing with a butane flame. The final object, approximately 5–6 cm in height, was introduced in the calorimeter cell previously described [20].

The calorimeter cell was filled with 5 ml of the liquid phase. An empty glass reference ampoule and the ampoule containing the lime, both sealed under vacuum, were placed inside the reference and measurement cells, respectively. Approximately 12 h was necessary to reach thermal equilibrium. The piston was then manually lowered, the curved tip of the ampoule was broken, and the powders were wetted by the liquid

phase. The heat flow was recorded with a frequency of one every 3 seconds for a total of 12 h. The return of flow curve to the initial values suggests that the reaction was completed within this time. The use of an empty ampoule in the reference cell is necessary to remove the mechanical effects of breaking the glass and the liquid entering the glass container. All of the tests were repeated three times, and an experimental error of less than 10% was obtained.

3) Nitrogen Adsorption Measurements At 78K

BET measurements [22] were performed using a symmetrical Sartorius microbalance described in detail previously [23]. Sample aliquots of approximately 100 mg were stored in a sealed container and placed in a platinum crucible inside the symmetrical thermobalance. The pressure was gradually lowered to a high vacuum level (10^{-3} Pa) at room temperature, and after the weight stabilised, an adsorption nitrogen isotherm at 78K was collected across the valid range of the BET equation ($0.05 < P/P^{\circ} < 0.35$). The experimental error of the surface area measurements was estimated to be approximately 3%.

4) Mercury Porosimeter

Mercury porosimetry of the samples was conducted using a Thermo Scientific porosimeter model Pascal 240 equipped with a standard dilatometer for powders.

5) SEM and EDAX

SEM-EDAX analyses of a carbon-coated sample were conducted using a SEM equipped with an X-ray dispersive analyser (Philips, EDAX PV 9100). The operating conditions were 20 kV, accelerating voltage and 2.20 nA beam current. The area of the EDAX analysis was of $4 \times 4 \mu\text{m}$.

Background to the Wetting Heat of Immersion

When solid particles, previously heat-treated in vacuum, are brought into contact with a pure wetting liquid the solid-liquid interactions can be quantitatively characterized in a simple and straightforward way with the measurement of the heat of immersion [18]. This exothermic heat of immersion accounts very reasonably for the formation of an adsorption layer several molecules thick on the surface of the particles. The kind of relationship between the particles wetting by the dispersing liquid molecules and the particle-particle adhesion play an important role in the formation of the solid-liquid interfaces and in the liberation of the exothermic heat of wetting. More exothermic is this effect more stable is the stability of the colloidal dispersion. The magnitude of the heat of wetting is a function of several variables. Among them the polarity of the dispersing liquid phase and the extent of hydrophobicity or hydrophilicity of the surfaces of the dispersed powders are very important. When these variables are set, the volume fraction θ of the dispersed solid phase, the shape and the dimension of the particles, single grains and/or clustered or sintered agglomerates, are all parameters that can account for the difference in the measured wetting heat values. On this ground when different set of powders, with almost equal surface chemistry, are wetted by the same liquid phase, it is possible to have information on the different morphologies of the dispersed microstructure units [22], through the comparison of the corresponding immersion calorimeter data and with the add of SEM analysis on the dried powders [17].

Usually the wetting heat of any solid-liquid dispersion is given in J/g of dispersed solid, but if the use of the immersion calorimeter is coupled with the determination of the BET surfaces of the starting dried powders the same parameter can be read as J/m². When one needs to compare the quality of products with equal average chemical composition but with different microstructure and surface properties, the definition of the exothermic heat of adsorption per square meter of dispersed particles is a more convenient definition [18]. To this parameter we gave the named of specific wetting heat and in this paper we'll refer to it with the symbol ξ .

Results and Discussion

Table 1 lists the starting limestones (LMST) pebbles, the decomposition temperatures, T_d , the corresponding lime powders obtained after 2.5 h of heating at constant temperature in air and their S_{BET} specific surface area. In the same table the data concerning the reagent grade of thermal decomposition of Calcite powders are reported.

TABLE 1. LIST OF STARTING LIMESTONES ROCKS DECOMPOSED AT DIFFERENT TEMPERATURE, IN AIR, FOR 2.5 H, TO OBTAIN DIFFERENT SET OF LIMES WITH S_{BET} SURFACE INDICATE IN COLUMN 4

Starting LMST rock peabbles	Decomposition temperature [°C]	Obtained limes	Limes S_{BET} (m ² /g)
LMST1	980	LM1 (980)	2.8
	1060	LM1(1060)	1.9
	1140	LM1(1140)	1.2
	1200	LM1(1200)	1.0
	1300	LM1(1300)	0.7
LMST2	980	LM2(980)	4.7
	1200	LM2(1200)	1.2
	1300	LM2(1300)	1
LMST3	1140	LM3(1140)	1.3
	1200	LM3(1200)	1.1
	1300	LM3(1300)	1
LMST4	1060	LM4(1060)	3.7
	1200	LM4(1200)	2.7
	1300	LM4(1300)	1.3
LMST5	980	LM5(980)	0.9
	1060	LM5(1060)	0.8
	1140	LM5(1140)	0.6
	1200	LM5(1200)	0.6
	900	CaO(900) r.g.	11
	1350	CaO(1350) r.g.	6.3

Fig. 1 Plots, as a matter of discussion, the decrease of the lime S_{BET} values vs. Td for the different limestone sources. Diamonds, squares, empty circles, solid circles and stars symbols are respectively referring to limes obtained from LMST1, LMST2, LMST3, LMST4, LMST5.

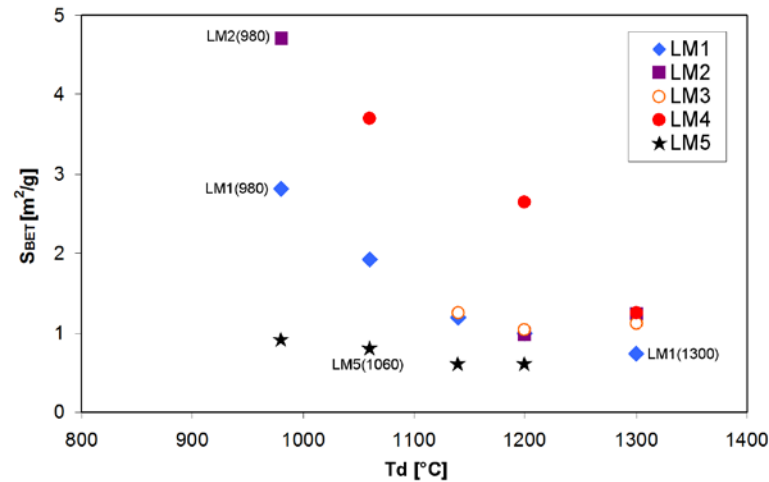


FIGURE 1. S_{BET} SPECIFIC SURFACE [M²/G] OF DIFFERENT LIMES, LM, OBTAINED FROM THE CALCINATION OF THE CORRESPONDING LIMESTONES, LMST, AT DIFFERENT DECOMPOSITION TEMPERATURE, TD, IN AIR.

In agreement with the catalytic effect of the escaping CO₂ on the sintering process of the CaO grains [5, 7], it can be observed that the surface area of the CaO obtained from the decomposition of CaCO₃ powders is always greater than the ones obtained from the decomposition of limestone pebbles, see Tab. 1. In fact CO₂ molecules which escape from the pebbles have to overcome more barriers than those emitted from a powder bed [3]. However, Fig. 1 clearly shows that, when the parent limestones are shaped in equal pebbles, the phenomenological law of the corresponding S_{BET} vs. Td curve is quite different. This result evidently accounts for the different internal texture of the limestones rocks [1] and their different impurity content.

To split the role of the internal rock texture from that of the impurities, explaining the experimental data S_{BET} vs Td (see Fig.1) of the corresponding limes, is a difficult, if not impossible task. However it is useful to compare the chemical analysis of the different limestones to gain some information. Tab. 2 allows to make such a comparison. It

is evident that only the LMST1 mineral rocks are characterized by a wt% of Al_2O_3 and SiO_2 definitely larger than the one present in all the others LMST samples.

TABLE 2. MAIN CHEMICAL COMPONENTS OF LMST ROCKS EXPRESS IN WEIGHT PERCENTAGE [%].

	LMST1	LMST2	LMST3	LMST4	LMST5
CaO	55.15	55.5	55.56	55.38	55.66
MgO	0.41	0.32	0.2	0.37	0.15
SiO ₂	0.24	0.05	0.1	0.06	0.05
Al ₂ O ₃	0.12	0.01	0.03	0.01	0.01
SrO	0.034	0.025	0.0256	0.0304	0.124
S	0.008	0.004	0.009	0.03	0.005
Fe ₂ O ₃	0.086	0.020	0.022	0.030	0.030
Na ₂ O	0.0083	0.0095	0.0031	0.0146	0.0021
MnO	0.0125	0.0081	0.0032	0.0014	0.0216
P ₂ O ₅	0.0007	0.0084	0.0022	0.0029	0.06
K ₂ O	0.0211	0.0019	0.0032	0.0033	0.002
TiO ₂	0.0043	0.0059	0.0017	0.0017	0.0039
C org	0.03	0.03	0.11	0.17	0.078
BaO	0.00052	0.00015	0.00029	0.00015	0.0029
V	0.00006	0.00007	0.00014	0.00011	0.00003
Zn	0.00012	0.0002	0.00029	0.00088	0.00028

In the literature it has been reported [24-26] that the addition of Al_2O_3 and SiO_2 oxides are useful to produces lime particles with an improved wear resistance in the plant [27] and perhaps to reduce the tendency of the lime particles to decrease their S_{BET} surface and porosity at high temperature and in presence of CO_2 . Those data cannot be extrapolated to infer that a similar role is played by the impurities of the mineral rocks in controlling the lime microstructure evolution during the thermal decomposition. In fact the impurity contents in the limestone matrix are very low in the average, but at the calcite grain boundaries their local concentration can be very high, and they can form small island and intrusion of minerals different from the host calcite [1]. Nevertheless the high wt% content of Al_2O_3 and SiO_2 in the LMST1 and LM1 samples, on account of the effect that these oxides have on the lime particle properties, are a signal that the LM1 particles might have chemical and physical properties different from those of other limes.

When the 20% of solid volume fraction of the lime powders, are dispersed in liquid paraffin, a colloidal system characterised by a percolate network, is formed [28, 29]. The percolate network is a dynamic structure due to bonds between microstructure units [19, 29, 30]. Since the paraffin molecules do not contain aromatic and naphthenic groups, only two forces are present: the attractive van der Waals forces and the steric repulsive forces at the solid-liquid interfaces formed between CaO surfaces and paraffin molecules. The formation of such interfaces implies an exothermic wetting heat, whose magnitude indicates the stability of the colloidal system [17].

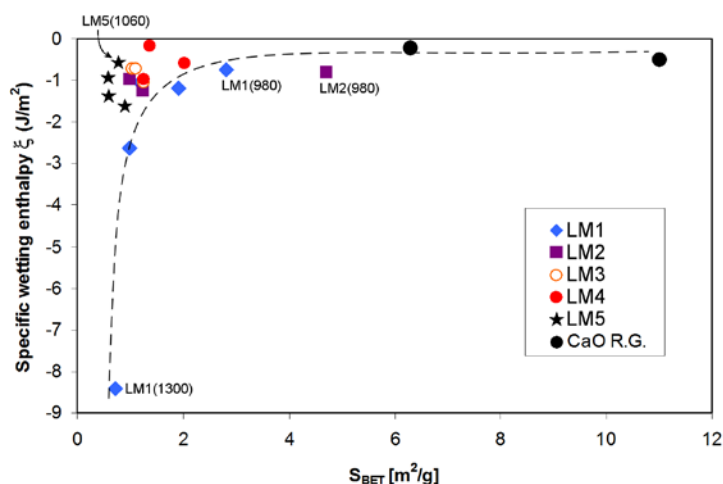


FIGURE 2. SPECIFIC WETTING HEAT, ξ [J/M²], OF DIFFERENT LM POWDERS IN LIQUID PARAFFIN AT THE TEMPERATURE OF 30°C, VS. THEIR S_{BET} [M²/G] SURFACES. FOR THE LIMES DESCRIBED IN THE TEXT ON THE GROUND OF SEM, EDAX AND HG POROSIMETER EXPERIMENTS, THE TEMPERATURE AT WHICH THEY HAVE BEEN OBTAINED, IS REPORTED NEAR TO THE SYMBOL.

Fig. 2 illustrates how the specific wetting heat, ξ , changes with the S_{BET} of limes obtained from thermal decomposition in air of different limestone rocks at different temperatures. The specific wetting heat of CaO oxides obtained from the decomposition of reagent grade calcite powders, are also reported for sake of comparison (solid black circles).

It is remarkable to observe that all the limes obtained from LMST2, LMST3, LMST3, LMST5 are characterized by an average ξ value equal to -0.9 ± 0.1 J/m², independent from their BET specific surface area values. But, surprisingly, only the limes derived from LMST1 show a dependence of ξ from their S_{BET} surface. For this family, when S_{BET} is equal to 0.7 ± 0.2 m²/g the corresponding ξ value is equal to -8 ± 2 J/m²; when S_{BET} is 2.8 ± 0.3 m²/g ξ approaches the value of -0.7 ± 0.1 J/m², very close to the one of the other sets of oxides.

All these values show that the interactions between the paraffin molecules and the CaO surfaces are weak [31], and strongly suggest that the dispersed microstructure units of the limes have a morphology quite similar to that observed in a detailed analysis of the dried powders [20].

The morphological results that will be illustrated and discussed in the following concerning two kind of limes from LMST2 and LMST5, have been confirmed also for all the oxides derived from LMST3, LMST4 and for the CaO from reagent grade of calcite powders.

Fig. 3 (a and b) shows typical SEM images, at the magnifications of 3000 \times (a) and 10000 \times (b), for the dried particles of LM2(980) limes, obtained from LMST2 at the temperature of 980°C. Fig. 4 (a and b) gives the same information for the limes LM5(1060) obtained from LMST5, at the temperature of 1060°C.

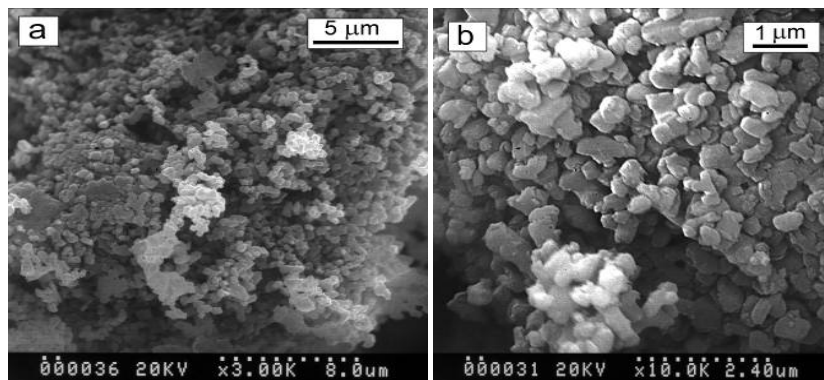


FIGURE 3. TYPICAL SEM IMAGES, AT THE MAGNIFICATION OF 3000 \times (PANEL A) AND AT 10000 \times (PANEL B) OF LM2(980). INDIVIDUAL NON POROUS GRAINS HAVE MAINLY POLYHEDRAL SHAPE WITH AVERAGE DIMENSION OF ABOUT 0.4 μm . S_{BET} SURFACE AREA IS EQUAL TO 4.5 ± 0.3 M²/G

In both images one can be observed the presence of aggregates among individual grains with a polyhedral shape and average size of 0.4 μm (Fig. 3b) and of 3 μm (Fig. 4b), respectively. By assuming spherical shape, the specific surface area that can be derived from these sizes, reads:

$$S_g = 3 / (\rho r) \quad (1)$$

where ρ is the powders density (g/cm³) and r is the particles radius (μm).

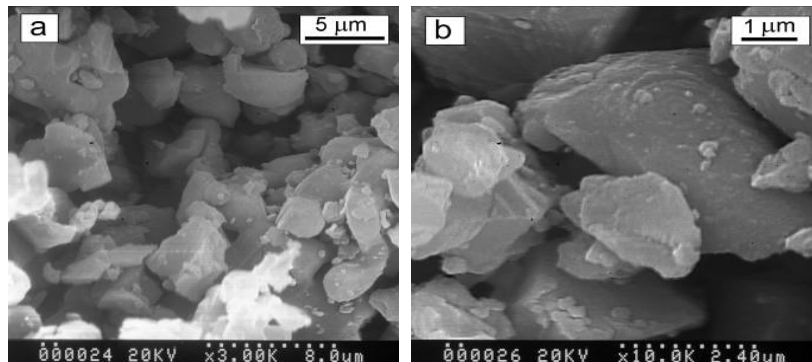


FIGURE 4. TYPICAL SEM IMAGES, AT THE MAGNIFICATION OF 3000 \times (PANEL A) AND AT 10000 \times (PANEL B) OF LM5(1060). THE INDIVIDUAL GRAINS ARE NOT POROUS, THE SHAPE IS IRREGULAR AND THE S_{BET} SURFACE IS EQUAL TO 0.6 ± 0.1 M²/G.

Application of equation (1) to the data of Fig. 3 and 4 yields S_g values of $4.5 \text{ m}^2/\text{g}$ for the sample LM2(980) and $0.6 \text{ m}^2/\text{g}$ for the sample LM5(1060), respectively. These values are very close to those obtained from the N_2 -adsorption data at 78 K, which lead to BET surface areas of 4.7 and of $0.8 \text{ m}^2/\text{g}$, respectively.

Thus, we can conclude that the lime individual grains are not porous, but the aggregates do. As a first approximation, pore aggregates can be assumed to have almost the same average size dimension as the individual grains [32, 33].

Since the paraffin molecules have an average size of 0.3 nm, they can penetrate inside the internal surfaces of both LM5(1060) and LM2(980) samples. More paraffin molecules can be accommodated in the sample of greater specific surface (LM2(980)), but if the surface “quality” of LM2(980) and LM5(1060) is such to give same interactions with the paraffin molecules, the specific wetting heat ξ , of both specimens is expected to be equal. The data reported in Fig. 2, confirmed this interpretation.

It is also interesting to observe the morphological shape of all lime aggregates. Closer observation of these data suggests that these shape are similar, despite the fact that they have different values of S_{BET} surface. This feature is also typical of the CaO aggregates obtained from R.G. CaCO_3 powders at 900°C and 1350°C , which are due to the catalytic action of the CO_2 , escaping from the reacting CaCO_3/CaO interfaces [34].

On this ground it can be inferred that although the LMST2, LMST3, LMST4, LMST5 are characterized by the presence of mineralogical impurities, these chemical compounds do not affect the formation of the shape of the corresponding lime aggregates.

All these evidences do not hold for the limes derived from LMST1 because, as Fig. 2 is clearly showing, their ξ value depend on the corresponding S_{BET} .

In seeking an explanation for this behaviour, let us compare morphological, EDAX and Hg porosimeter data concerning the limes LM1(980) and LM1(1300) obtained from the same source as LMST1 at the temperatures of respectively 980°C and 1300°C .

Fig. 5 (panel a and b) shows a comparison between pore volume and pore size distribution of sample LM1(980) and LM1(1300). It can be observed that total pore volume of sample LM1(980) is $0.55 \text{ cm}^3/\text{g}$, higher than that of the LM1(1300) limes, which amounts to $0.15 \text{ cm}^3/\text{g}$. The pore size distribution of the LM1(980) sample is in the range between 0.1 and $0.6 \mu\text{m}$, while the one of the limes LM1(1300) ranges between 0.3 and $3 \mu\text{m}$. All these data, including the comparison of S_{BET} value for the sample LM1(1300) ($0.7 \text{ m}^2/\text{g}$) and LM1(980) ($2.8 \text{ m}^2/\text{g}$), can be explained on the ground that the sample LM1(980) has been obtained at 980°C , while the LM1(1300) limes was produced at 1300°C .

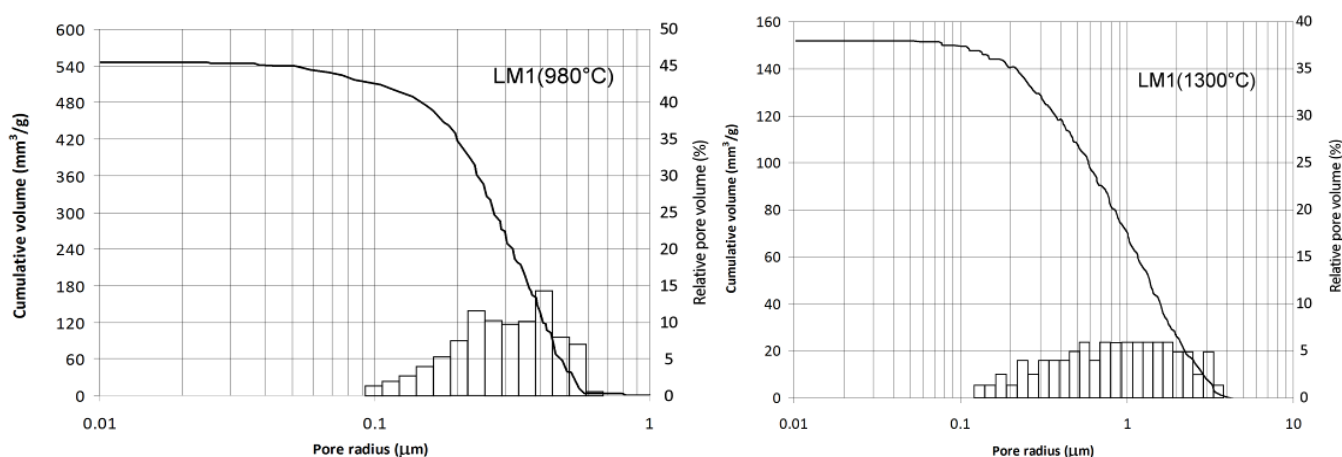


FIGURE 5. HG INTRUSION CURVES FOR AGGREGATES OF LM1(980) GRAINS, PANEL A, AND FOR LM1(1300) GRAINS, PANEL B. THE TOTAL POROSITY DECREASE FROM $0.55 \text{ cm}^3/\text{g}$ (980) TO $0.15 \text{ cm}^3/\text{g}$ (1300). THE PORES RADII FOR THE INTRUSION OF THE HG IN THE AGGREGATES RANGE FROM 0.1 AND $0.6 \mu\text{m}$ IN LM1(980) AND FROM 0.3 AND $3 \mu\text{m}$ IN LM1(1300).

Fig. 6 (a and b) and Fig. 7 (a and b) illustrate typical SEM images for LM1(980) (see Fig. 6), and LM1(1300) (see Fig. 7) particles and agglomerates. As observed, the morphology of the LM1(980) sample is similar to the ones of the

limes obtained from LMST2, LMST3, LMST4, LMST5. Correspondingly this lime has a specific wetting heat, equal to -0.7 ± 0.1 J/m², which is included in the average value of -0.9 ± 0.1 J/m² of limes with independent from their surface area. But the morphologies of the LM1(1300) sample (see Fig. 7) are quite different and are characterized by a complex set of individual grains, some having polyhedral shape with average size dimension of 0.5 μ m, others being flat and large particles with $10 \times 10 \times 1$ μ m size.

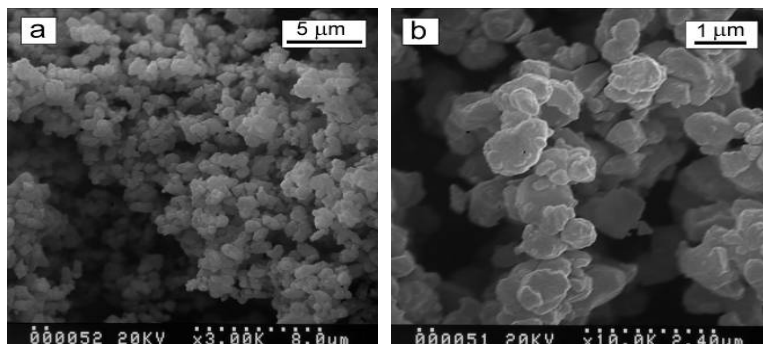


FIGURE 6. TYPICAL SEM IMAGES, AT THE MAGNIFICATION OF 3000 \times (PANEL A) AND AT 10000 \times (PANEL B) OF LM1 OBTAINED FROM LMST1 AT 980°C. AGGREGATES OF INDIVIDUAL GRAINS OF ABOUT 1 μ m ARE PRESENT AS THE ONES OBSERVED FOR LM2 (980). S_{BET} SURFACE AREA IS EQUAL TO 2.8 ± 0.3 M²/G.

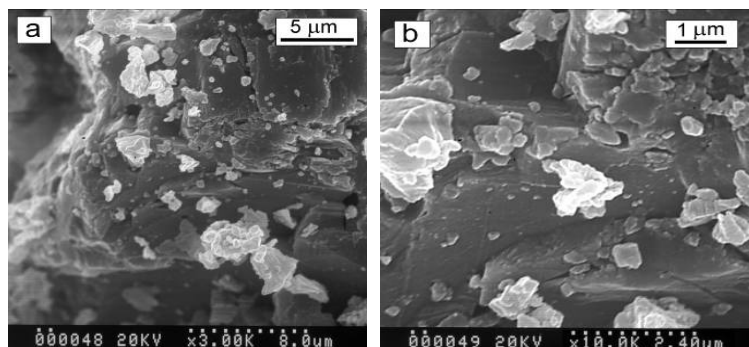


FIGURE 7. TYPICAL SEM IMAGES, AT THE MAGNIFICATION OF 3000 \times (PANEL A) AND AT 10000 \times (PANEL B) OF LM1 OBTAINED FROM LMST1 AT 1300°C. LARGE AND FLAT INDIVIDUAL GRAINS WITH AVERAGE DIMENSION OF 10 μ m \times 1 μ m ARE CHARACTERIZING THE SAME LM1 SAMPLE BECAUSE THE TEMPERATURE OF DECOMPOSITION OF THE LMST1 ROCKS HAS BEEN RAISED FROM 980°C (SEE FIG.6) TO 1300°C. S_{BET} SURFACE AREA IS 0.7 M²/G.

These morphological changes, cannot be due only to the effects of the LMST1 decomposition temperature. Indeed, when lime grains evolve from a round and/or polyhedral shape to a flat one, others high temperature processes must occur [1], beside the ones due to the gas-solid reaction associated with the escaping CO₂ [7, 35].

Fig. 8 (a and b) shows the EDAX spectrum of two statistical meaningful powders of limes LM1(980) and LM1(1300) taken at room temperature on oxides that have been produced from the same LMST1 rocks at the temperature of 980°C, LM1(980), and at 1300°C, LM1(1300). The comparison between the two spectra has been done by setting equal the peaks of the Ca K reflection. Within the experimental limits of this kind of analysis [36], when the decomposition temperature of LMST1 is raised from 980°C to 1300°C the peaks concerning the Na element disappear, while the zone between the Mg and Fe elements seems somewhat to reduce its height. It is interesting to observe that the reflections due to the Al and Si elements appear more enhanced at 1300°C than at 980°C.

Given the presence of Al₂O₃ and SiO₂ impurities in the starting LMST1 rocks (see Tab. 2), it is possible that a small amount of aluminates-silicates compound be present in the matrix of the LMST1 rocks because of its geological history.

The phase diagram CaO-Al₂O₃-SiO₂ [37] evidences that a liquid eutectic phase exists at the temperature of 1347°C with a composition of 55% in CaO, 45% in Al₂O₃ and 10% in SiO₂. This composition might be present as impurities locally in the LMST1 matrix due to its geological history. If so, when the decomposition temperature, become 1300°C, the mobility of the atoms in such a phase should be so high as to produce a viscous liquid phase that might change the shape of most CaO grains. At the temperature of 980°C no changes in the shape of the CaO grains as well as in the surface chemical nature are possible, because the formation of the viscous calcium-

aluminates-silicates phase is not feasible from a thermodynamic point of view [37].

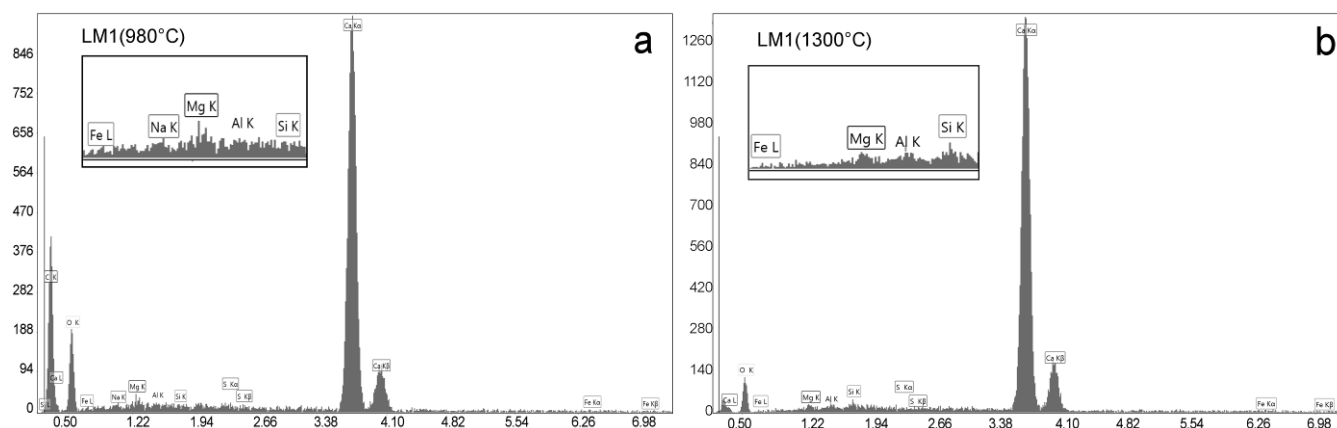


FIG. 8. EDAX SPECTRUM FOR LM1 POWDERS OBTAINED FROM THE DECOMPOSITION OF LMST1 AT 980°C (PANEL A) AND 1300 °C (PANEL B). THE WINDOWS ARE AN ENLARGEMENT PORTION OF THE SPECTRUM. AS THE LMST1 DECOMPOSITION TEMPERATURE IS RAISED, THE CORRESPONDING LIME, PANEL B, DOES NOT SHOWS THE PEAK FOR THE NA, WHILE THE REFLECTIONS FOR AL AND SI APPEAR MORE DEFINED.

As a consequence the limes from LMST2, LMST3, LMST4, LMST5 are not characterized by grain agglomerates with flat morphologies because the amount of Al_2O_3 and SiO_2 in the starting rocks is almost negligible in comparison with the ones of the LMST1.

Since the paraffin molecules interact with the lime surfaces only under the action of the van der Waals and steric forces, and since the paraffin does not contain aromatic and naphthenic groups, any change in the chemical nature of the lime surface introducing acid-basic attractions [31] is not felt by the paraffin molecules. Thus, for each lime, the value of it is a thermodynamic parameter that is only linked to the morphology of the particle aggregates, which in turn are dependent upon the limestone impurity content and upon their thermal decomposition conditions.

Conclusions

In this paper, we have focused on a new application of the immersion calorimeter method, to find an average macroscopic parameter, the specific wetting heat, ξ , that can be related with the shape of the lime microstructure units dispersed in liquid paraffin.

These morphologies are dependent upon the thermal decomposition conditions under which the limes have been produced and upon the nature of the impurities in the starting rocks.

The impurities influencing the shape of individual and agglomerated lime particles, according to this study are represented by SiO_2 and Al_2O_3 .

At the temperature of 1300°C these impurities present a high mobility of Ca, Si, and Al atoms due to the possible pre-existing and/or formation of calcium-aluminates-silicates compounds which form a viscous liquid-like phase. Due to the presence of this viscous phase, the shape of the oxides grains can dramatically change. From rhombohedra and/or spherical CaO grains ranging between 0.4 and 3 μm , the particle shape is changing into flat and large crystallites of 10 x 10 x 1 μm .

The average macroscopic thermodynamic parameter ξ , i.e. the specific wetting heat [J/m^2] determined through the immersion calorimetric technique, is able to give information on the limes particle morphologies, provided that the scout molecules interacting with the CaO surfaces, are bonded by van der Waals and steric forces, like in the case of liquid paraffin.

From a technological point of view these results can be used to optimise the thermal decomposition conditions of limestone rocks to obtain limes with proper surface and microstructure qualities, starting from limestone rocks sources with selected content of impurities.

ACKNOWLEDGMENT

This paper is in memory of Prof. Alan W. Searcy of the University of California, Berkeley: a scientist that highlighted this research field through his thermodynamic and kinetic studies in the high-temperature gas-solid reactions field.

This study is based on unresolved scientific questions that originated from technological researches made on the ground of a contract between the Lhoist Recherche et Développement S.A., Belgium, and the Civil, Chemical and Environmental Dept. (DICCA, former DICheP) of the University of Genoa, Italy. The authors wish to thank the Lhoist Co., the students and technicians of the Material Engineering Laboratory, that have been involved in these research topic. The interest of Prof. A. Converti and Prof. M. Capurro of the University of Genoa (DICCA), has been appreciated.

REFERENCES

- [1] Beruto, D.T., Botter, R., Cabella, R., and Lagazzo, A. "A consecutive decomposition-sintering dilatometer method to study the effect of limestone impurities on lime microstructure and its water reactivity". *J. Eur. Ceram. Soc.* 30(6) (2010) 277–286.
- [2] L'vov, B.V., Polzik, L.K., and Ugolkov, V.L. "Decomposition kinetics of calcite: a new approach to the old problem". *Thermochim. Acta* 390 (2002) 5–19
- [3] Beruto, D.T., Searcy, A.W., and Kim, M.G. "Microstructure, kinetic, thermodynamic analysis for calcite decomposition: free surface and powder bed experiments". *Thermochim. Acta* 424 (2004) 99–109.
- [4] Powell, E.K., and Searcy, A.W. "Surface-areas and morphologies of CaO produced by decomposition of large CaCO_3 crystal in vacuum". *J. Am. Ceram. Soc.* 65 (1982) c42–c44
- [5] Borgwardt, R.H. "Calcination kinetics and surface area of dispersed limestone particles". *AIChE J.* 31 (1985) 103–110.
- [6] Fuller, E.L., and Yoos, T.R. "Surface properties of limestones and their calcination products". *Langmuir* 3 (1987) 753–760.
- [7] Beruto, D.T., Barco, L., and Searcy, A.W. " CO_2 -catalyzed area and porosity changes in high-surface-area CaO aggregates". *J. Am. Ceram. Soc.* 67(7) (1984) 512–5.
- [8] Shearer, J.A., Johnson, I., and Turner, C.B. "Interaction of NaCl with limestones during calcination". *J. Am. Ceram. Soc.* 59 (1980).
- [9] Lagazzo, A., Nortier, P., and Botter, R. "The effect of alkaline cations on the operation of the Kraft recovery and other kilns". *ATIP Pates Kraft* 66(1) (2012)
- [10] Beruto, D.T., Lagazzo, A., Botter, R., and Finocchio, E. "Calcium oxides for CO_2 capture obtained from the thermal decomposition of CaCO_3 particles coprecipitated with Al^{3+} ions". *J. Eur. Ceram. Soc.* 32 (2012) 307–315.
- [11] Flügel, E. "Microfacies of carbonate rocks. Analysis, interpretation and applications". Springer, 2004, ISBN 3–540–22016–X.
- [12] Salvador, C., Lu, D., Anthony, E.J., and Abanades, J.C. "Enhancement of CaO for CO_2 capture in an FBC environment", *Chem. Eng. J.* 96 (2003) 187–195.
- [13] Fennel, P.S., Davidson, J.F., Dennis, J.S., and Hayhurst, A.N. "Regeneration of sintered limestone sorbents for the sequestration of CO_2 from combustion and other systems". *J. Energy Inst.* 80(2) (2007) 116–118.
- [14] Abanades, J.C., Anthony, E.J., Lu, D.Y., Salvador, C., and Alvarez, D. "Capture of CO_2 from combustion gases in a fluidised bed of CaO". *AIChE J.* 50 (2004) 1614–1622.
- [15] Hughes, R.W., Lu, D., Anthony, E.J., and Yu, Y. "Improved long-term conversion of limestone-derived sorbents for in situ capture of CO_2 in a fluidized bed combustor". *Ind. Eng. Chem. Res.* 43(18) (2004) 5529–5539.
- [16] Alvarez, D., and Abanades, J.C. "Pore-size and shape effects on the recarbonation performance of calcium oxide submitted to repeated calcination/recarbonation cycles". *Energ. Fuels* 19 (2005) 270–278.
- [17] Király, Z. "Calorimetric methods for the study of adsorption of surfactants at solid/solution interfaces", in: M. Dekker, *Thermal Behaviour of Dispersed Systems*, New York, 2001, Chap. 9.
- [18] Dékány, I., and Nagy, L.G. "Immersional wetting and adsorption displacement on hydrophilic/hydrophobic surfaces". *J.*

- Colloid Interf. Sci. 147(1) (1991) 119–128.
- [19] Sevick, E.M., and Ball, R.C. "Dilute heteroaggregation: A description of critical gelation using a cluster-cluster aggregation model". *J. Colloid Interf. Sci.* 144(2) (1991) 561–570.
- [20] Beruto, D.T., Lagazzo, A., and Botter, R. "Silica-paraffin and kaolin-paraffin dispersions: Use of rheological and calorimetric methods to investigate the nature of their dispersed microstructure units". *Colloids Surface A* 396 (2012) 153–160.
- [21] Napper, D.H. "Polymeric Stabilization of Colloidal Dispersions". Academic Press, New York, 1983.
- [22] Beruto, D.T., Lagazzo, A., and Botter, R. "Nanosopic water layers adsorbed onto mesoporous silica aggregates and their effect on the stability and the static yield stress of their dispersion in liquid paraffin". *Colloids Surface A* 407 (2012) 133–140.
- [23] Brunauer, S., Emmett, P.H., and Teller, E. *J. Am. Chem. Soc.* 60 (1938) 309.
- [24] Beruto, D.T., Botter, R., and Searcy, A.W. "H₂O catalyzed sintering of 2-nm-crosssection particles of MgO". *J. Am. Ceram. Soc.* 70(3) (1987) 155–159.
- [25] Manovic, V., and Anthony, E.J. "Long-term behavior of CaO-based pellets supported by calcium aluminate cements in a long series of CO₂ capture cycles". *Ind. Eng. Chem. Res.* 48 (19) (2009) 8906–12.
- [26] Aihara, M., Nagai, T., Matsushita, J., Negishi, Y.I., and Ohya, H. "Development of porous solid reactant for thermal-energy storage and temperature upgrade using carbonation / decarbonation reaction". *Appl. Energy* 69 (2001) 225–38.
- [27] Li, Z.S., Cai, N.S., Huang, Y.Y., and Han, H.J. "Synthesis, experimental studies and analysis of a new calcium-based carbon dioxide sorbent". *Energy Fuels* 19 (2005) 1447–52.
- [28] Lin, M.Y., Klein, R., Lindsay, H.M., Weitz, D.A., Ball, R.C., and Meakin, P. "The structure of fractal colloidal aggregates of finite extent". *J. Colloid Interf. Sci.* 137 (1) (1990) 263–280.
- [29] Beruto, D.T., Lagazzo, A., Botter, R., and Grillo, R. "Yield stress measurements and microstructure of colloidal kaolin powders clusterized and dispersed in different liquids". *Particuology* 7(6) (2009) 438–444.
- [30] Quemada, D. "Rheological modelling of complex fluids. I. The concept of effective volume fraction revisited". *Eur. Phys. J. Appl. Phys.* 1 1 (1998) 119–127.
- [31] Drago, R.S., and Wayland, B.B. "A Double-Scale Equation for Correlating Enthalpies of Lewis Acid-Base Interactions". *J. Am. Chem. Soc.* 87(16) (1965) 3571–3577.
- [32] Boyton, R.S. "Chemistry and Technology of Lime and Limestone". 2nd ed., Wiley-Interscience, New York, 1980.
- [33] Kingery, W.D., Bowen, H.K., and Uhlmann, D.R. "Introduction to Ceramics", 2nd ed., John Wiley & Sons, 1976.
- [34] Borgwardt, R.H. "Calcium oxide sintering in atmosphere containing water and carbon dioxide". *Ind. Eng. Chem. Res.* 28 (1989) 493–500.
- [35] Borgwardt, R.H. "Sintering of nascent calcium oxide" *Chem. Eng. Sci.* 44(1) (1989) 53–60.
- [36] Goldstein, J.I., Newbury, D.E., Echlin, P., Joy, D.C., Fiori, C., and Lifshin, E. "Scanning Electron Microscopy and X-Ray Microanalysis". Plenum, New York, 1992.
- [37] Osborn, and E.F., Muan, A. "Phase equilibrium diagrams of oxides systems". Plate 1, *Am. Ceram. Soc. & Ceram. Found.* (1960).

Dario T Beruto is formerly ordinary professor of material science at University of Genoa, Italy. He received his degree in Chemical Engineering at the Faculty of Engineering of Genoa in 1966. He was visiting scientist at the University of California, Berkeley (USA) during 1970–1972. From 1972 to 1983, he was lecturer and assistant professor in applied solid-state physical chemistry and from 1983 to 1986 he was associate professor in materials science at Faculty of Engineering, University of Genoa. He obtained the chair of full professor in material science in 1986. Professor Beruto joined the American Ceramic Society in 1974 and he has been member of the Advisory Committee for the European Ceramic Society Conferences. He has been a member of the Academy of Ceramics since 1991. Professor Beruto has written approximately 150 papers as author and co-author and has six patents.

Rodolfo Botter graduated in Chemical Engineering at the Faculty of Engineering of Genoa (Italy). Since 2003 is associate professor of Materials Science at the University of Genoa. He published over 40 scientific contributions in international journals in the field of the ceramic materials and biomedical area. He is co-author of many conference proceedings and of three patents.

Alberto Lagazzo graduated in Chemical Engineering at the Faculty of Engineering of Genoa (Italy) in 2007 and received his PhD in Materials Science at the University of Genoa in 2010. At the present, he is post doc researcher at the Department of Civil, Chemical and Environment (DICCA) of the University of Genoa, dealing of solid-liquid dispersions and ceramic materials. He is co-author of over 10 papers and many conference proceedings.